

**Supporting Information**

to

**Size-dependent interaction of amyloid  $\beta$  oligomers with brain total lipid  
extract bilayer – fibrillation vs. membrane destruction**

Dusan Mrdenovic,<sup>1,2</sup> Marta Majewska,<sup>1</sup> Izabela S. Pieta,<sup>1</sup> Piotr Bernatowicz,<sup>1</sup> Robert Nowakowski,<sup>1</sup> Włodzimierz Kutner,<sup>1,3</sup> Jacek Lipkowski,<sup>2</sup> Piotr Pieta<sup>1,\*</sup>

<sup>1</sup>Institute of Physical Chemistry, Polish Academy of Sciences, Kasprzaka 44/52, 01-224 Warsaw, Poland

<sup>2</sup>Department of Chemistry, University of Guelph, 50 Stone Road East, Guelph, Ontario N1G 2W1, Canada

<sup>3</sup>Faculty of Mathematics and Natural Sciences, School of Sciences, Cardinal Stefan Wyszyński University in Warsaw, Wóycickiego 1/3, 01-815 Warsaw, Poland

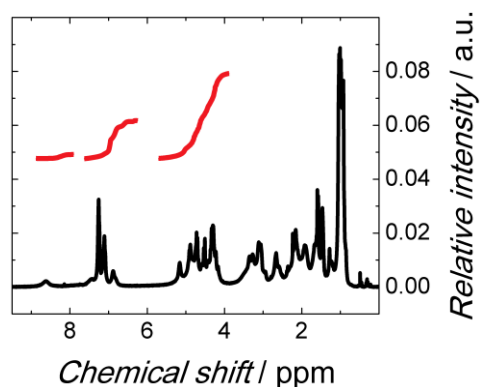


**Figure S1.** The  $^1\text{H}$  NMR spectrum of the A $\beta$  in deuterated trifluoroacetic acid.

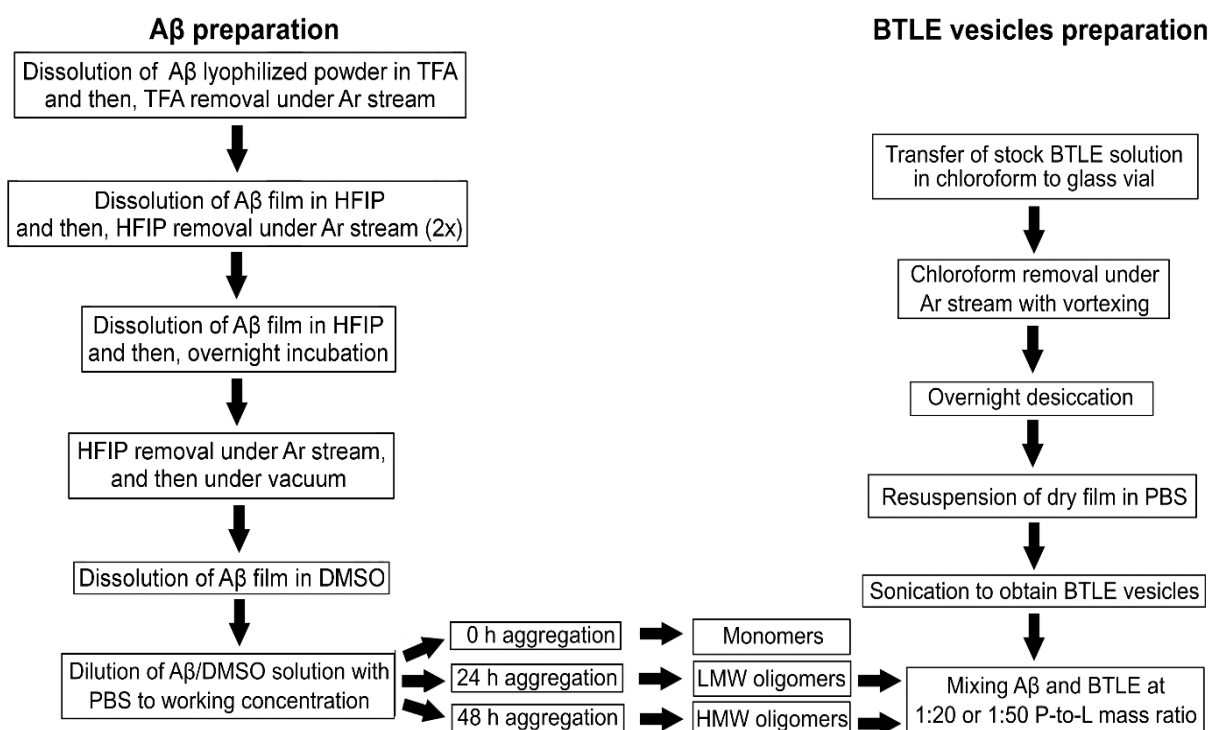


**Figure S2.** The flowchart describing the experimental steps for preparing solutions of A $\beta$ , BTLE vesicles, and A $\beta$ -BTLE mixture.

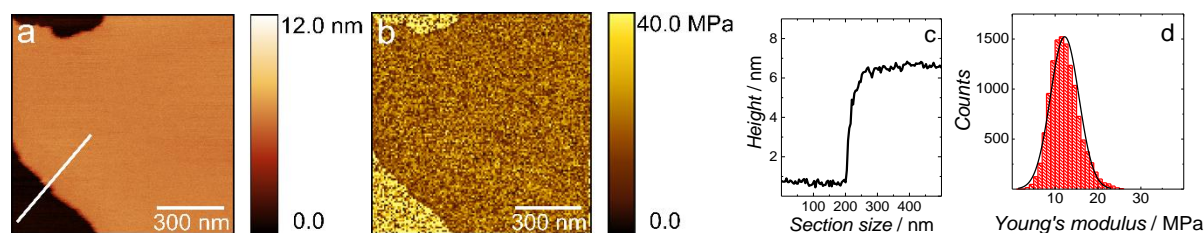


**Figure S3.** (a) The AFM topography image and (b) corresponding Young's modulus map of the BTLE supported lipid bilayer on mica in the 0.01 M PBS (pH = 7.4) solution acquired at 21°C. (c) Cross-sectional profile of the membrane measured along the line shown in Panel a. (d) Histogram showing Young's modulus distribution determined from 12 000 FD curves collected for different points of the bilayer shown in Panel b.

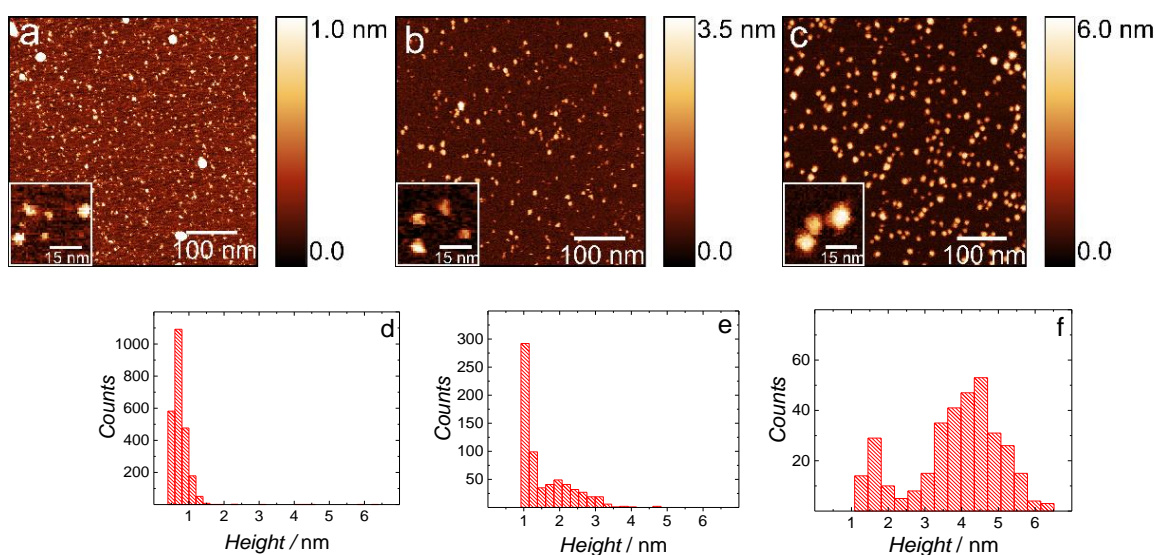


**Figure S4.** AFM topography images in air of (a) A $\beta$  monomers as well as (b) LMW and (c) HMW A $\beta$  oligomers deposited on the mica surface. Insets exhibit magnified parts of the corresponding topography images showing the shape of the aggregates into greater detail. Histograms of corresponding height distribution of (d) A $\beta$  monomers as well as (e) LMW and (f) HMW A $\beta$  oligomers. The aggregates were formed in the PBS-DMSO solution in the BTLE vesicles absence.

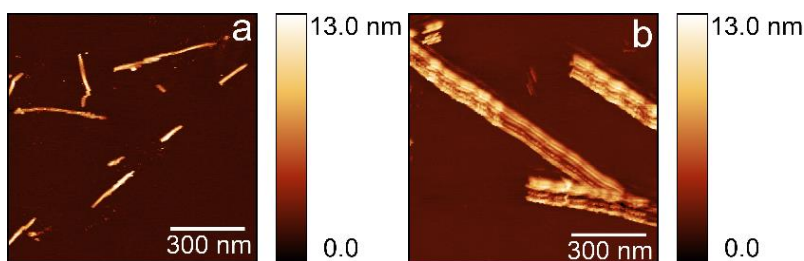


**Figure S5.** The AFM topography image of A $\beta$  (a) protofibrils and (b) fibrils deposited on the mica surface.

**AFM tip characterization.** Diameter and quality of the AFM tips used were estimated by using a well-established procedure. This procedure consists in imaging the Ti roughness sample (Bruker) and analyzing the obtained image (Figure S6a) using Tip Qualification option in NanoScope Analysis software. This analysis resulted in constructing a software model of the tip (Figure S6b) and determining effective tip diameters (ETDs) at different distances from the tip apex (Figures S6c and S6d). The tip characterization analysis showed that ETDs were 8.5 and 26.3 nm at the 3 and 20 nm distance, respectively, from the tip apex (Figure S6e). In Figure S5f it is illustrated how ETD is calculated based on tip cross section.

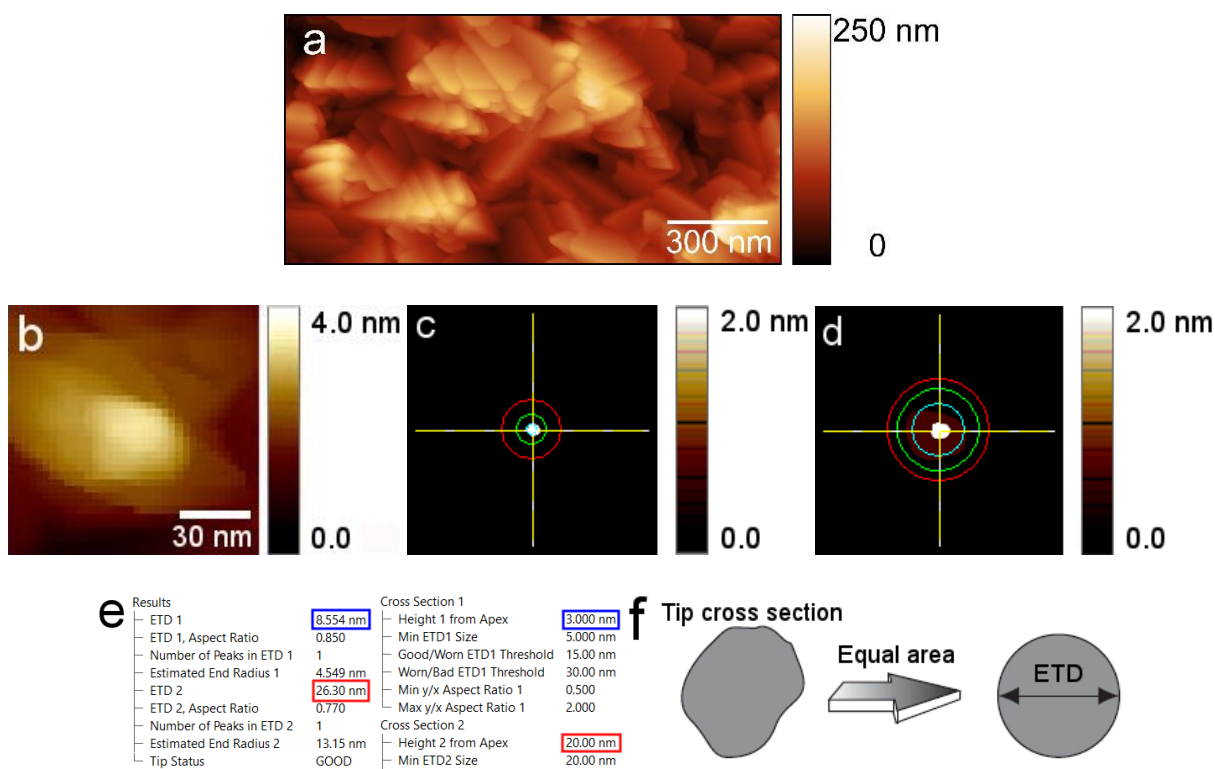


**Figure S6.** (a) The AFM topography image of a Ti roughness sample used for the tip radius and quality determination. (b) The top-view image of the software model of the tip. Cross-section diagrams showing the size and shape of the tip at the distance of (c) 3 and (d) 20 nm from the tip apex. (e) Results of the tip radius and quality determination. (f) Scheme of the effective tip diameter calculation from the tip cross section.

The ETD limits the ability of the tip to measure the depth of pores. That is, the tip will not be able to reach the bottom of the pore if the diameter of the tip is larger than the diameter of the pore. Consequently, the pore depth cannot be determined. Therefore, it is important to determine whether the tip is sufficiently sharp to be used for measuring the depth of the pores in the BTLE bilayer. We analyzed pores formed in the inner leaflet of the BTLE lipid bilayer (Figure 4a) by measuring diameters and depths of the big, middle, and small size pores. Green, cyan, and blue arrows in the magnified region of the inner leaflet of the BTLE lipid bilayer shows big, middle, and small size pores, respectively (Figure S7a). Cross-sectional profile of the BTLE bilayer shows that bilayer thickness is 6.1 ( $\pm 0.3$ ) nm (Figure S3c). This result would suggest that thickness of a single leaflet is  $\sim 3$  nm. Based on the tip characterization analysis, it is determined that the tip diameter at the distance of 3 nm from its apex was 8.5 nm. If the pore diameter exceeds 8.5 nm, the tip is capable of reaching bottom of the 3-nm deep pore. Therefore, it can measure the depth of the pores formed in a single leaflet. This is because the depth of these pores does not exceed 3 nm as thickness of a single leaflet is 3 nm. Figure S7b shows the relation between the measured depth and diameter of pores analyzed. Apparently, the measured pore depths did not exceed 2 nm if the pore diameter was smaller than 10 nm. On the other hand, the pore depth ranged from 2.5 up to 3.5 nm if pore diameter was larger than 10 nm. This result suggests that diameter of small pores was smaller than the tip diameter and the tip could not measure depths deeper than 2 nm. Presumably, this is a reason why small distribution of depths for small pores was obtained. On the other hand, the tip was capable of measuring a real depth in case of mid and big holes, and this is why wide distribution of depths was observed.

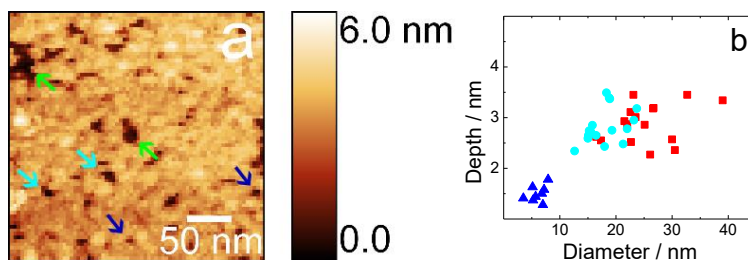


**Figure S7.** (a) The AFM topography image showing pores in the inner leaflet of the BTLE lipid bilayer. (b) Correlation between depth and diameter of (■) big, (●) mid and (▲) small pores.

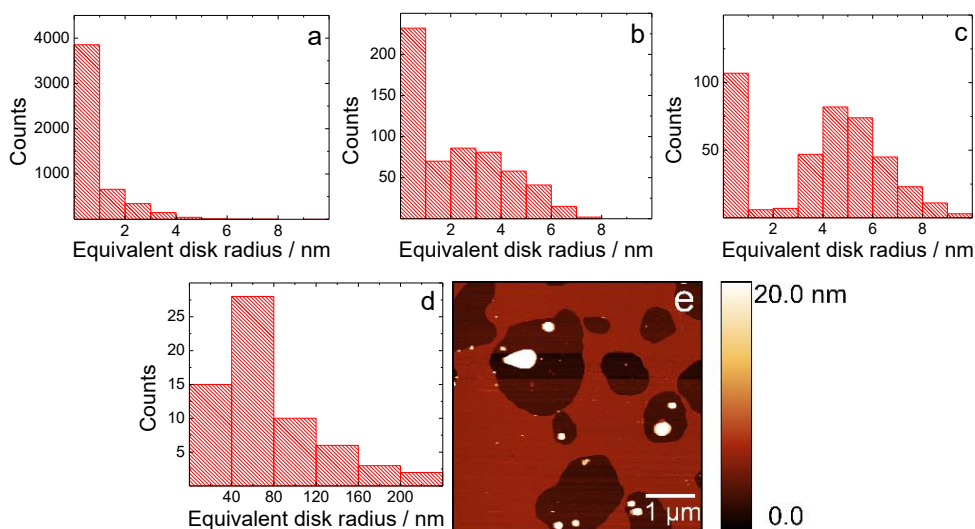


**Figure S8.** Histograms showing equivalent disk radii distribution of (a) A $\beta$  monomers, (b) LMW A $\beta$  oligomers, (c) HMW A $\beta$  oligomers and (d) BTLE vesicles. (e) The AFM topography image showing unfused BTLE vesicles and the BTLE lipid bilayer deposited on the mica support.

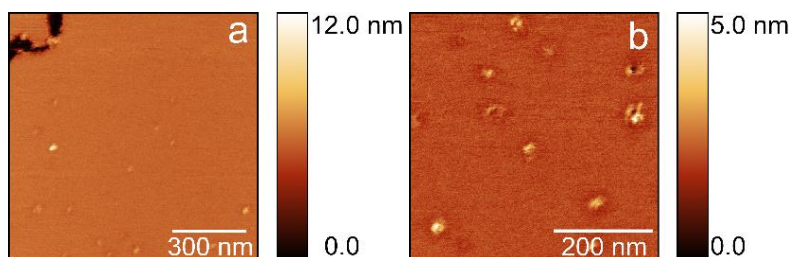


**Figure S9.** (a, b) The AFM topography images showing larger area of the pores in the supported BTLE bilayer formed by LMW A $\beta$  oligomers in 0.01M PBS (pH=7.4).

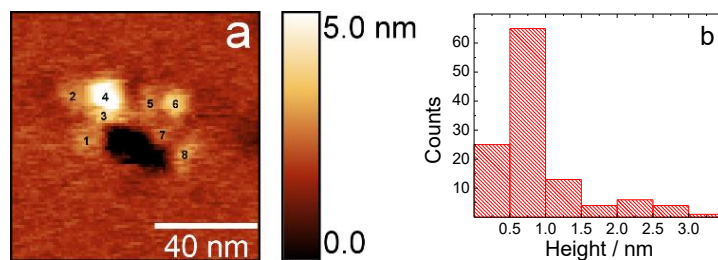


**Figure S10.** (a) AFM topography image of the BTLE bilayer in 0.01 M PBS (pH = 7.4) with the pore surrounded by eight A $\beta$  oligomers. (b) Histogram showing protrusion distribution of the LMW A $\beta$  oligomers above the BTLE bilayer.



**Movie MS1.** Movie of a single pore expansion and A $\beta$  oligomers insertion into the BTLE lipid bilayer.



**Movie MS2.** Movie of a multiple pore expansion and A $\beta$  oligomers insertion into the BTLE lipid bilayer.

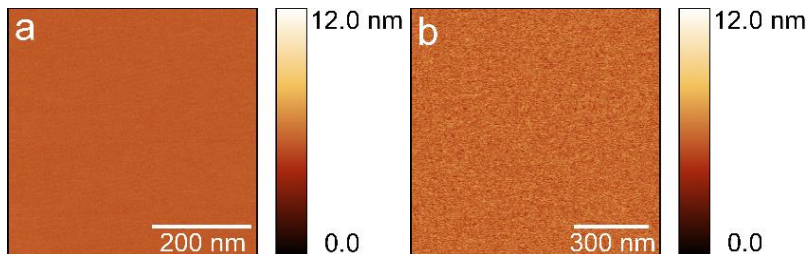


**Figure S11.** AFM topography images of the supported BTLE bilayer in 0.01 M PBS (pH = 7.4) showing film topography in the absence of LMW A $\beta$  oligomers at (a) 0 and (b) 72 h.